INTERNATIONAL JOURNAL FOR NUMERICAL METHODS IN FLUIDS, VOL. 7, 1191–1209 (1987)

2-D/3-D FINITE-ELEMENT SOLUTION OF THE STEADY EULER EQUATIONS FOR TRANSONIC LIFTING FLOW BY STREAM VECTOR CORRECTION*

FADI EL DABAGHI, OLIVIER PIRONNEAU

INRIA, Le Chesnay—University of Paris VI, France

AND

JACQUES PERIAUX AND GÉRARD POIRIER

Avions Marcel Dassault/Bréguet Aviation, St Cloud, France

SUMMARY

In this paper we study the validation of the new formulation (potential-stream vector) of the steady Euler equations in 2-D/3-D transonic lifting regime flow. This approach, which is based on the Helmholtz decomposition of a velocity vector field, is designed to extend the potential approximation of Euler equations for severe situations such as high transonic or rotational subsonic flows. Different results computed by a fixed point algorithm on the stream vector correction are shown and discussed by comparing them with those obtained by the full potential approach.

KEY WORDS Helmholtz Decomposition Euler Finite Element Transonic Rotational Potential Stream Vector

INTRODUCTION

The full potential approach is still one of the simplest and most attractive methods to solve the steady Euler equations in the following two very useful cases:

(1) subsonic regime with no vorticity or entropy on the upstream boundary
(2) transonic regime with weak shocks and no upstream vorticity or entropy.

When shocks are strong or vorticity is non-zero on the upstream boundary, we introduce the Helmholtz decomposition of a vector field into a gradient of a scalar potential ϕ plus a curl of a stream vector ψ. ψ will be interpreted as a correction to the potential flow in order to generalize the full potential model for solving the steady Euler equations in most subsonic and transonic cases. This new formulation leads to a fixed point algorithm for ψ; the main ingredients of this algorithm are the following:

(1) a least-squares method to compute ϕ by solving the non-linear potential equation
(2) a characteristics method to compute the shocks and to transport the entropy, the helicity and the enthalpy
(3) a $\mathbb{P}^1$ finite-element method to compute ψ.

* Based on a contributed paper

0271–2091/87/111191–19$09.50

In the first section, we present the motivation and the objectives of this work. In the second section, we recall the theoretical aspects of the Helmholtz decomposition[1,2] of $(\mathbf{L}^2(\Omega))^3$ into two orthogonal subspaces and how to use it for deriving a $(\phi-\psi)$ formulation of the steady Euler equations. In the third section, we introduce a fixed point algorithm associated with the new formulation; we discuss in detail the shock detection step and we describe briefly the rest of the numerical tools involved in this algorithm. In the final section, numerical flow simulations—transonic lifting/non-lifting regime around 2-D/3-D NACA0012 profiles and wings for severe test cases—are presented in order to improve the robustness and the validity of the methodology.

MOTIVATION

For simplicity, we consider the following two classical cases which are very useful in numerical aerodynamics applications:

(1) an external flow (Figure 1) around a portion of wing between two parallel walls, where the regime is supposed transonic
(2) an internal flow (Figure 2) in a nozzle, where the upstream boundary conditions of the vorticity (resp. the entropy) are non-zero (resp. non-constant).

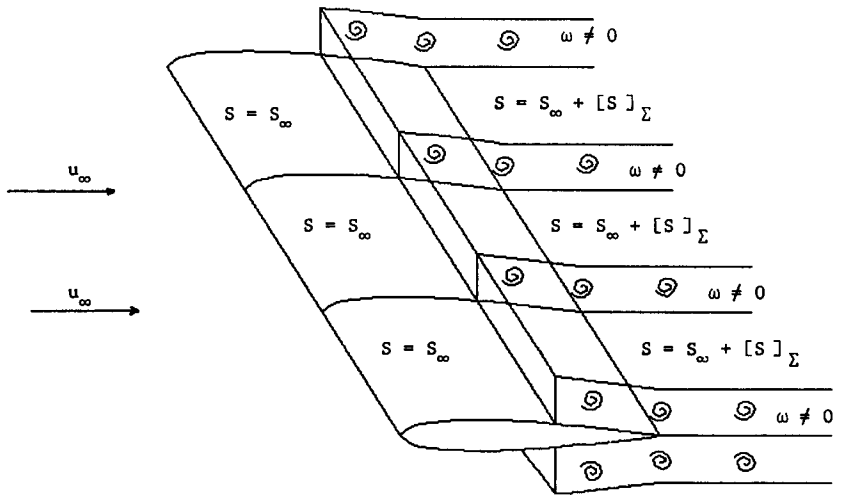

Figure 1

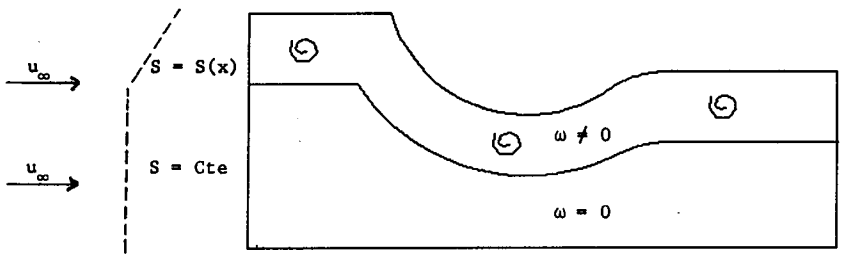

Figure 2

We denote by $[\mathbf{v}]_\Sigma$ the jump of the variable $\mathbf{v}$ across the discontinuity Σ.
Generally, steady flows are described by the continuity equation

$$\nabla\cdot(\rho\mathbf{u}) = 0. \tag{1}$$

In the transonic regime with weak shocks or in the subsonic regime with an upstream boundary condition of vorticity close to zero and under the hypothesis of isentropic perfect gas law, these flows governed by (1) are usually well approximated by the equation

$$\nabla\cdot((H - |\nabla\phi|^2/2)^{1/\gamma-1}\nabla\phi) = 0, \tag{2a}$$

known as the 'potential transonic equation', which can be written as

$$\nabla\cdot(\rho\,\nabla\phi) = 0, \tag{2b}$$

where H is given and the velocity assumed as a curl free vector field, i.e.

$$\mathbf{u} = \nabla\phi, \quad \boldsymbol{\omega} = \nabla\times\mathbf{u} = 0. \tag{3}$$

More precisely, the assumption (3) means that the entropy S is constant in the flow or its jump across the shock Σ is close to zero (the rotational effects are neglected). But unfortunately, as shown in the first example for external flow, if the regime is a high transonic one, a strong shock appears and S is no longer constant and its jump is no longer small; similarly, in the second example for internal flow, the non-zero upstream boundary conditions of the vorticity make the entropy non-constant in the flow. So through these two examples we observe the non-validity of the potential hypothesis (3) because the rotational effects are not taken into account by the model; then (2a) or (2b) is not available in such cases and as mentioned before, since $\boldsymbol{\omega} = \nabla\times\mathbf{u}$ is not small, we shall use the Helmholtz decomposition of the velocity

$$\mathbf{u} = \nabla\phi + \nabla\times\boldsymbol{\psi} \tag{4}$$

in order to generalize the potential approach (2) for severe situations, where $\boldsymbol{\psi}$ will take into account the rotational part of the flow.

The main idea of the new formulation is to use (4) in (1) and then to solve the modified potential equation

$$\nabla\cdot(\rho\,\nabla\phi) = -\nabla\rho\cdot\nabla\times\boldsymbol{\psi}. \tag{5}$$

In fact (5) will be solved iteratively where we suppose ρ to be a known function of $\mathbf{u}$ at each iteration. The stream vector $\boldsymbol{\psi}$ involved in the second member of (5) will be calculated as the solution of

$$\nabla\times\nabla\times\boldsymbol{\psi} = \boldsymbol{\omega}(=\nabla\times\mathbf{u}), \tag{6}$$

where $\boldsymbol{\omega}$ is a simple algebraic expression obtained after some transformations on the Euler equations as explained in the next section. We assume for a first guess that the velocity is known, and then by solving (5)–(6) iteratively the velocity will be updated by (4) at each step, and so on. The system (5)–(6) describes the (ϕ–$\boldsymbol{\psi}$) formulation.

THE (ϕ–$\boldsymbol{\psi}$) FORMULATION

Before the description of the (ϕ–$\boldsymbol{\psi}$) formulation, we recall briefly some theoretical aspects of the Helmholtz decomposition (4) detailed in References 1 and 2. The fundamental problem is to define a set of suitable boundary conditions on ϕ and $\boldsymbol{\psi}$ yielding the uniqueness of such a decomposition. In fact the principal difficulty concerns the boundary conditions on $\boldsymbol{\psi}$, as explained

by the following. By taking respectively the divergence and the curl of (4), we obtain

$$\Delta\phi = \nabla\cdot\mathbf{u} \tag{7}$$

and

$$\nabla \times \nabla \times \boldsymbol{\psi} = \nabla \times \mathbf{u}. \tag{8}$$

Then, by adding to (7) one of the two Neumann boundary conditions (this choice was guided by physical considerations easily understood if we remark that our goal is to extend the potential approach), we obtain

$$(\partial\phi/\partial n)|_\Gamma = \mathbf{u}\cdot\mathbf{n}|_\Gamma \tag{9a}$$

or

$$(\partial\phi/\partial n)|_\Gamma = 0. \tag{9b}$$

Equations (9a) and (9b) imply respectively the two non-standard boundary conditions on $\boldsymbol{\psi}$ (but natural from a physical point of view),

$$(\nabla \times \boldsymbol{\psi})\cdot\mathbf{n}|_\Gamma = 0 \tag{10a}$$

and

$$(\nabla \times \boldsymbol{\psi})\cdot\mathbf{n}|_\Gamma = \mathbf{u}\cdot\mathbf{n}|_\Gamma. \tag{10b}$$

Equations (10a) and (10b) will be replaced respectively by the two standard boundary conditions on $\boldsymbol{\psi}$ (but not natural from a physical point of view),

$$\boldsymbol{\psi} \times \mathbf{n}|_\Gamma = 0 \tag{11a}$$

and

$$\boldsymbol{\psi} \times \mathbf{n}|_\Gamma = \boldsymbol{\psi}_d \times \mathbf{n}|_\Gamma, \tag{11b}$$

which is a straightforward application of the Green's formula

$$\int_\Gamma (\mathbf{v} \times \mathbf{n})\cdot\nabla w \, d\sigma = -\int_\Gamma (\nabla \times \mathbf{v})\cdot\mathbf{n} w \, d\sigma, \quad \forall w \in \mathbf{H}^1(\Omega), \quad \mathbf{v} \in (\mathbf{H}^1(\Omega))^3, \tag{12}$$

where $\boldsymbol{\psi}_d$ must satisfy

$$(\nabla \times \boldsymbol{\psi}_d)\cdot\mathbf{n}|_\Gamma = \mathbf{u}\cdot\mathbf{n}|_\Gamma. \tag{13}$$

Formally, the problem (7)–(9) on ϕ in the 2-D or 3-D cases is well posed in $\mathbf{H}^1(\Omega)/\mathbb{R}$. On the other hand, while the 2-D problem (8)–(11) defines a unique $\boldsymbol{\psi}$ in $\mathbf{H}^1(\Omega)$, the 3-D one does not define $\boldsymbol{\psi}$ even up to a constant because the operator $\nabla \times \nabla \times$ is a strongly elliptic operator only on the solenoidal vector spaces. This last condition, detailed in Reference 3, is justified by the following operator identity:

$$\nabla \times \nabla \times \boldsymbol{\psi} = -\Delta\boldsymbol{\psi} + \nabla(\nabla\cdot\boldsymbol{\psi}), \quad \forall \boldsymbol{\psi}. \tag{14}$$

Remark 1. In 2-D, the ellipticity condition of $\nabla \times \nabla \times$ is automatically satisfied because $\boldsymbol{\psi}$ is orthogonal to the fluid motion and has only one component, so its divergence is zero. By another way, the boundary conditions (11a) and (11b) on $\boldsymbol{\psi}$ become respectively $\boldsymbol{\psi}|_\Gamma = 0$ and $\boldsymbol{\psi}|_\Gamma = \boldsymbol{\psi}_d|_\Gamma$. In 3-D, $\boldsymbol{\psi}$ has three components, which do not represent stream lines.

Since our purpose is to generalize the full potential approach, we will consider only (7)–(9a) and (8)–(11a) as stated by the following theorem.

Theorem. Let Ω be a bounded open domain of $\mathbb{R}^3$, simply connected; let Γ be its boundary C^1-differentiable and C^2-piecewise ($\Gamma = U_{i=1}\Gamma_i$, Γ_i being the connected component of Γ). Let

$\mathbf{u}$ be a given vector field in $(\mathbf{L}^2(\Omega))^3$. Let ϕ and ψ be respectively the unique solutions of the problems

$$(\nabla\phi, \nabla w) = (\mathbf{u}, \nabla w), \quad \forall w \in \mathbf{H}^1(\Omega)/\mathbb{R}, \quad \phi \in \mathbf{H}^1(\Omega)/\mathbb{R} \tag{15}$$

$$(\nabla \times \psi, \nabla \times \mathbf{v}) + (\nabla \cdot \psi, \nabla \cdot \mathbf{v}) = (\mathbf{u}, \nabla \times \mathbf{v}), \quad \forall \mathbf{v} \in \mathbf{V}, \quad \psi \in \mathbf{V}, \tag{16}$$

where

$$\mathbf{V} = \left\{ \mathbf{v} \in (\mathbf{H}^1(\Omega))^3 : \mathbf{v} \times \mathbf{n}|_\Gamma = 0, \int_{\Gamma_i} \mathbf{v} \cdot \mathbf{n} \, d\sigma = 0, \forall \Gamma_i \right\}.$$

Then

$$\mathbf{u} = \nabla\phi + \nabla \times \psi \quad \text{and} \quad \nabla \cdot \psi = 0 \tag{17}$$

and the decomposition (17) is unique in $\{\mathbf{H}^1(\Omega)/\mathbb{R}\} \times \{\mathbf{V}\}$. (The proof is detailed in References 1 and 2.)

The other alternative given by (7)–(9b) and (8)–(11b) is also discussed in References 1 and 2, and we mention quickly that the difficulty in this case is caused by a Laplace–Beltrami problem on Γ associated with (13) to determine ψ_d; for technical reasons the equivalent theorem stated in this case requires more regularity on the vector $\mathbf{u}$, namely $\nabla \mathbf{u} \in \mathbf{L}^2(\Omega)$, and a flux condition on Γ_i. The variational formulation on ψ is quite similar, the difference being that $(\psi - \psi_d) \in \mathbf{V}$.

Remark 2. Problem (16) has a unique solution because the bilinear form in (16) defines an inner product on $\mathbf{V}$ (cf. Reference 2). Then if $\mathbf{u}$ represents a velocity vector field describing a transonic flow for example, ϕ will be the scalar potential describing the general aspects of the flow and ψ will be the stream vector describing the rotational part of the fluid.

This remark will be very useful, because if the vorticity tend to zero, it yields ψ tending also to zero. Indeed

$$(\nabla \times \psi, \nabla \times \mathbf{v}) + (\nabla \cdot \psi, \nabla \cdot \mathbf{v}) = 0, \quad \forall \mathbf{v} \in \mathbf{V}, \ \psi \in \mathbf{V} \tag{18}$$

and by the last remark we obtain $\psi \equiv 0$ and $\mathbf{u} = \nabla\phi$; we find again the potential formulation. So ψ can be used as a rotational correction to the potential via the theorem in high transonic or rotational subsonic flows.

Remark 3. In 2-D, $\mathbf{V} = \mathbf{H}_0^1(\Omega)$; i.e. $\mathbf{H}^1(\Omega)$ with zero trace on Γ.

Now let us describe the $(\phi$–$\psi)$ process; at first and as mentioned in the previous section, the main idea involves computing ψ by solving (8), which implies known vorticity in order to update the velocity by (17). To determine ω we suppose for a first guess a potential solution given by $\mathbf{u} = \nabla\phi$ calculated by solving (2b), and after this recall of the steady Euler equations for inviscid flow and the thermodynamical relations linking the variables involved in these equations we will describe how to compute ω:

$$\nabla \cdot (\rho \mathbf{u}) = 0 \qquad \text{(mass conservation)}, \tag{19}$$

$$\nabla \cdot (\rho \mathbf{u} \otimes \mathbf{u}) + \nabla p = 0 \qquad \text{(momentum conservation)}, \tag{20}$$

$$\nabla \cdot (\rho E \mathbf{u} + p\mathbf{u}) = 0 \qquad \text{(energy conservation)}, \tag{21}$$

$$p = \rho^\gamma S \qquad \text{(state gas law)}, \tag{22}$$

$$\nabla \cdot (\rho s \mathbf{u}) \geqslant 0 \qquad \text{(second thermodynamic principle)}, \tag{23}$$

where

$$S = e^{S/C_V}, \tag{24a}$$

$$E = H - p/\rho, \tag{24b}$$

$$H = \tfrac{1}{2}|\mathbf{u}|^2 + [\gamma/(\gamma - 1)]p/\rho. \tag{24c}$$

Combining (19) and (24c) in (20), leads to

$$\rho \nabla H - \rho \mathbf{u} \times \boldsymbol{\omega} - [\rho^{\gamma}/(\gamma - 1)] \nabla S = 0. \tag{25}$$

Then, by taking the cross product of (25) with $\mathbf{u}$, we find an new algebraic formula for the vorticity given by

$$\boldsymbol{\omega} = \lambda \rho \mathbf{u} + \frac{\mathbf{u}}{|\mathbf{u}|^2} \times \left(\frac{\rho^{\gamma - 1}}{\gamma - 1} \nabla S - \nabla H \right), \tag{26}$$

where the scalar λ (close to the helicity) is defined by

$$\lambda = \frac{\boldsymbol{\omega} \cdot \mathbf{u}}{\rho |\mathbf{u}|^2}. \tag{27}$$

So through (26) we observe that determining $\boldsymbol{\omega}$ needs H, S, λ and ρ as known variables. We remedy this situation by noticing that $\boldsymbol{\omega}$ is solenoidal ($\nabla \cdot \boldsymbol{\omega} = 0$) and this leads to a transport equation for λ:

$$\rho \mathbf{u} \cdot \nabla \lambda = -\nabla \cdot \left[\frac{\mathbf{u}}{|\mathbf{u}|^2} \times \left(\frac{\rho^{\gamma - 1}}{\gamma - 1} \nabla S - \nabla H \right) \right] \tag{28}$$

where H, S and ρ are determined by the classical relations obtained easily as follows. Using (19) and (24b) in (21), we obtain the transport equation for H:

$$\mathbf{u} \cdot \nabla H = 0. \tag{29}$$

Taking the inner product of (26) with $\mathbf{u}$ and using (29) we derive also a transport equation for S:

$$\mathbf{u} \cdot \nabla S = 0. \tag{30}$$

Finally, by using (22) in (24c), a simple equation for ρ is obtained:

$$\rho = \frac{[(\gamma - 1)(H - \frac{1}{2}|\mathbf{u}|^2)]^{1/(\gamma - 1)}}{\gamma S}. \tag{31}$$

At this point H, S, ρ and λ can be computed in sequence successively from (29), (30), (31) and (28), then $\boldsymbol{\omega}$ is determined by (26) and thus the rotational correction ψ can be calculated by solving (8)–(11a); finally $\mathbf{u}$ can be updated via (17) by solving the modified potential equation (5).

Remark 4. The equations derived for S, λ, ρ and $\boldsymbol{\omega}$ are not valid across shocks; we have to add locally the Rankine–Hugoniot conditions detailed in Reference 1, which give the jump value of such variables through the discontinuities.

METHOD OF SOLUTION

From the above considerations described in the first section, we introduce the following fixed point algorithm on ψ operating for the 2-D/3-D general situation.

Step 0. For initialization we consider an isentropic potential flow in order to compute a first guess for $\mathbf{u}^0$ as follows: $\psi^0 = 0$, $S^0 = S_\infty$, $H^0 = H_\infty$, $\lambda^0 = \lambda_\infty$ ($_\infty$: at upstream infinity). Compute $\mathbf{u}^0 = \nabla \phi^0$ by solving the full potential equation (2) and then ρ^0 by (31). We order the equations to be solved as described by the following steps:

Step 1. Solve $\mathbf{u}^m \cdot \nabla H^{m+1} = 0$ in Ω with $H^{m+1}|_{\Gamma_{in}} = H^m|_{\Gamma_{in}} \Rightarrow H^{m+1}$.

Step 2. Solve $\mathbf{u}^m \cdot \nabla S^{m+1} = 0$ in Ω with $S^{m+1}|_{\Gamma_{in}} = S^m|_{\Gamma_{in}} \Rightarrow S^{m+1}$.

Step 3. Solve (28) in Ω with $\lambda^{m+1}|_{\Gamma_{in}} = \lambda^m|_{\Gamma_{in}}$ (in the 2-D case, $\lambda = 0$) $\Rightarrow \lambda^{m+1}$.

Step 4. Compute $\boldsymbol{\omega}^{m+1}$ by (26) $\Rightarrow \boldsymbol{\omega}^{m+1}$.

Step 5. Solve $\nabla \times \nabla \times \boldsymbol{\psi}^{m+1} = \boldsymbol{\omega}^{m+1}$ in Ω with (11a) on $\Gamma \Rightarrow \boldsymbol{\psi}^{m+1}$.

Step 6. Solve $\nabla \cdot \rho^m(|\mathbf{u}^m|) \nabla \phi^{m+1} = -\nabla \rho^m \cdot \nabla \times \boldsymbol{\psi}^{m+1}$ in Ω with (9a) on $\Gamma \Rightarrow \phi^{m+1}$.

Step 7. Update $\mathbf{u}^{m+1}$ by (4) and ρ^{m+1} by (31) $\Rightarrow \mathbf{u}^{m+1}$, ρ^{m+1}. $m = m+1$, go to Step 1 until convergence of the rotational correction.

Before the description of the numerical methods involved in this algorithm, we shall introduce some classical definitions to clarify the discretization. Let Ω_h be a polygonal approximation of Ω; we shall use the simple $\mathbb{P}^1$ finite element for discretization; let $\mathbf{T}_h$ be a regular triangulation of Ω_h:

$$\mathbf{T}_h = \cup \{T_k\}, \quad k = 1, \text{NT (NT: number of tetrahedra/triangles; NS: number of nodes)}$$

In the following, we will describe the methods used in the above algorithm.

Transport of H, S and λ

Let v_- and v_+ be the upstream and downstream value of a variable v on the shock surface Σ. The transport equations involved in Steps 1, 2 and 3 are of the type

$$\mathbf{u} \cdot \nabla \mathbf{a} = f \tag{32}$$

where $\mathbf{u}$ and f are given on $\mathbf{T}_h$. This transport model equation has an analytical solution given by

$$\mathbf{a}(x) = a_\infty(X_\infty) + \int_{\sigma^\infty}^{0} f(X(\sigma))\, d\sigma + a_+(X_\Sigma) - a_-(X_\Sigma), \quad x \in \Omega \tag{33}$$

where σ is the curvilinear variable of the stream line $C(x)$ that passes through x. $C(x)$ is defined by the curve $X(\cdot)$

$$\frac{dX}{d\sigma} = \mathbf{u}(X(\sigma)), \quad \sigma \in]\sigma_\infty, 0[, \quad X(\sigma_\infty) = X_\infty \quad \text{and} \quad X(0) = x, \tag{34}$$

where X_∞ and X_Σ are respectively the intersection of $C(x)$ with the upstream boundary Γ_{in} and the shock surface Σ. Since $\mathbf{u}$ is P_0 on $\mathbf{T}_h$, $C(x)$ is a broken line, where each piece represents the direction of $\mathbf{u}$ in a $\{T_k\} \in \mathbf{T}_h$ crossed by $C(x)$, i.e.

$$C(x) = \bigcup_{i=1}^{N-1} [x^i, x^{i+1}], \quad x^1 = x, \quad x^N = X_\infty \tag{35}$$

and N is the number of $\{T_k\} \in \mathbf{T}_h$ crossed by $C(x)$. The vertices $\{x^i\}_{i=2}^N$ of $C(x)$ are computed as follows:

$$\text{find} \quad t^i > 0 \quad \text{such that} \quad x^i = x^{i-1} - t^i \mathbf{u}|_{T_k}, \tag{36}$$

where x^i and x^{i-1} are one the frontier of $\{T_k\}$ and t^i represents an artificial time; we note that system

(36) describes the flow going upstream and x^N is reached when the characteristic arrives at the upstream infinity Γ_{in}. By another way, if system (36) is written in terms of the barycentric coordinates $\{\mu_j\}_{j=1,4}$ of x^i in $\{T_k\}$, it becomes easier to compute t^i and to find the next element $\{T_1\}$ adjacent to $\{T_k\}$; indeed, (36) leads to

$$\sum_{j=1}^{4} \mu_j q^j = \sum_{j=1}^{4} \aleph_j q^j - t^i \mathbf{u}|_{T_k}, \quad t^i > 0, \tag{37}$$

where $\{\aleph_j\}_{j=1,4}$ are the barycentric coordinates of x^{i-1} in $\{T_k\}$ and $\{q^j\}_{j=1,4}$ are the global coordinates of the nodes of $\{T_k\}$. We add to equation (37) the following constraints:

$$\sum_{j=1}^{4} \mu_j = \sum_{j=1}^{4} \aleph_j = 1, \quad \mu_j \geqslant 0, \quad \aleph_j \geqslant 0 \tag{38a}$$

$$\exists \alpha, \beta \in \{1,2,3,4\}, \quad \alpha \neq \beta \quad \text{such that} \quad \mu_\alpha = 0 \quad \text{and} \quad \aleph_\beta = 0 \quad (\text{if } x^{i-1} \neq x^1). \tag{38b}$$

To solve problem (37)–(38) we first introduce a new variable $\{\xi_j\}_{j=1,4}$ defined by

$$\xi_j = (\mu_j - \aleph_j)/t^i, \quad j = 1,4 \tag{39}$$

and then we rewrite the system (37)–(38) according to the new unknowns:

$$\sum_{j=1}^{4} \xi_j q^j = -\mathbf{u}|_{T_k}, \quad \sum_{j=1}^{4} \xi_j = 0. \tag{40}$$

System (40) is a (4 × 4) simple linear system solved quickly to determine $\{\xi_j\}_{j=1,4}$. Then by using (38b) with an elimination process we compute $\{\mu_j\}_{j=1,4}$ of x^i, and by the same technique we determine $\{T_1\}$ adjacent to $\{T_k\}$ to start up again from x^i to find x^{i+1} in $\{T_1\}$, and so on. This last step has to be done carefully in order to avoid jamming and particularly to detect Σ by testing the Mach number on $\{T_k\}$ and $\{T_1\}$ in order to compute a_+ and a_- given by the Rankine–Hugoniot conditions.

Remark 5. The relative simplicity of the analytical concept of the characteristics method is not comparable with the discretization difficulties encountered during the computation. These difficulties are essentially due to:

(1) the non-zero divergence of the computed transport velocity field (which poses the interface problems on the elements)
(2) the slip boundary conditions on Γ_B are satisfied in a weak sense in the solution of the modified potential equation (5)
(3) the round-off errors (for more details see Reference 4).

This method of characteristics is not dissipative and unconditionally stable in a finite-element context (see Reference 5). We are actually developing an adaptive mesh algorithm in 2-D by defining a new triangulation generated by the vertices taken on the curves $C(x_\alpha)$, where $\{x_\alpha\}$ are choosen previously on Γ_{out}. The new mesh following the stream lines will be concentrated only around special areas (for example, shock surfaces and lift linest in order to reduce the number of nodes of the triangulation and to obtain best precision of calculations.

Calculation of the stream vector ψ

Since ω is computed in Step 4 by (26), equation (6) involved in Step 5 is equivalent to the variational problem

$$(\nabla \times \boldsymbol{\psi}, \nabla \times \mathbf{v}) + (\nabla \cdot \boldsymbol{\psi}, \nabla \cdot \mathbf{v}) = (\boldsymbol{\omega}, \mathbf{v}), \quad \forall \mathbf{v} \in \mathbf{V}, \quad \boldsymbol{\psi} \in \mathbf{V}. \tag{41}$$

This formulation is discretized by classical $\mathbb{P}^1$ piecewise linear functions (see References 1 and 2); we introduce the space $\mathbf{V}_h$ as an approximation of $\mathbf{V}$ in the sense that, $\forall \mathbf{v} \in \mathbf{V}$, there exists a $\mathbf{v}_h \in \mathbf{V}_h$ such that

$$\|\mathbf{v} - \mathbf{v}_h\|_{1,\Omega} \leqslant Ch, \tag{42}$$

where C is a positive constant and h is the greatest element edge length. We denote respectively by NI and NF the number of interior and boundary nodes (NS = NI + NF). The space $\mathbf{V}_h$ can be defined as

$$\mathbf{V}_h = \left\{ \boldsymbol{\psi}_h(x) = \sum_{i=1}^{\mathrm{NI}} \boldsymbol{\psi}_j^i w^i(x) \mathbf{e}^j + \sum_{i=\mathrm{NI}+1}^{\mathrm{NS}} \xi^i w^i(x) \mathbf{n}^i \right\} \tag{43}$$

with $\mathbf{n}^j$ the unitary normal defined on the node j, $w^i(x)$ the classical $\mathbb{P}^1$ piecewise linear functions, and $\boldsymbol{\psi}^i$ defined by

$$\boldsymbol{\psi}^i = \begin{cases} \displaystyle\sum_{i=1}^{3} \boldsymbol{\psi}_j^i \mathbf{e}^j, & \text{the value of } \boldsymbol{\psi}_h \text{ at the interior node } i \\ \xi^i \mathbf{n}^i, & \text{the value of } \boldsymbol{\psi}_h \text{ at the boundary node } i. \end{cases} \tag{44}$$

The discretized problem of (41) is equivalent to solving a linear system in $\mathbb{R}^{3\mathrm{NI}+\mathrm{NF}}$ computed by a preconditioned conjugate gradient algorithm; as indicated on Figure 3, this system has very nice features for CPU time and for memory storage.

$\mathbf{F}^i$ represents the second member of (41); $\mathbf{D}$, $\mathbf{B}$ and $\mathbf{E}$ are the block matrices defined by

$$\mathbf{D}_{ij} = (\nabla w^i, \nabla w^j), \quad 1 \leqslant i, j \leqslant \mathrm{NI}, \tag{45}$$

$$\mathbf{B}_{ij}^k = \mathbf{D}_{ij} \mathbf{n}_k^j, \quad k = 1, 2, 3, \quad 1 \leqslant i \leqslant \mathrm{NI}, \quad \mathrm{NI} + \mathbf{I} \leqslant j \leqslant \mathrm{NS}, \tag{46}$$

$$\mathbf{E}_{ij} = \mathbf{n}^i \mathbf{n}^j \mathbf{D}_{ij} + (\mathbf{n}^i \times \mathbf{n}^j) \cdot \int_\Omega \nabla w^i \times \nabla w^j \, dx, \quad \mathrm{NI} + 1 \leqslant i, j \leqslant \mathrm{NS}. \tag{47}$$

$\mathbf{D}$ and $\mathbf{E}$ are calculated once and stored in Morse form as a one-dimensional problem and $\{\mathbf{n}^i\}_{i=\mathrm{NI}+1,\mathrm{NS}}$ are also stored to construct $\mathbf{B}$ when it is needed.

Remark 6. In the 2-D case, problem (41) becomes a simple Dirichlet one as follows:

$$(\nabla \boldsymbol{\psi}, \nabla \mathbf{v}) = (\boldsymbol{\omega}, \mathbf{v}), \quad \forall \mathbf{v} \in \mathbf{V}, \quad \boldsymbol{\psi} \in \mathbf{V}. \tag{48}$$

Calculation of the scalar potential ϕ

The potential and modified potential equations (2b)–(5) involved in Step 0 and 6 are treated similarly by a least-squares method detailed in References 6–8. Notice that the uniqueness of a

$$\begin{array}{cccccc} & \mathrm{NI} & \mathrm{NI} & \mathrm{NI} & \mathrm{NF} & \\ \mathrm{NI} & \mathbf{D} & \mathbf{0} & \mathbf{0} & \mathbf{B}^1 & \boldsymbol{\psi}_1^i \\ \mathrm{NI} & \mathbf{0} & \mathbf{D} & \mathbf{0} & \mathbf{B}^2 & \boldsymbol{\psi}_2^i \\ \mathrm{NI} & \mathbf{0} & \mathbf{0} & \mathbf{D} & \mathbf{B}^3 & \boldsymbol{\psi}_3^i \\ \mathrm{NF} & \mathbf{B}^1 & \mathbf{B}^2 & \mathbf{B}^3 & \mathbf{E} & \xi^i \end{array} = \mathbf{F}_i$$

Figure 3. Linear system associated with the discretized $\nabla \times \nabla \times$ operator

physical solution is achieved by upwinding the density in the flow direction when shocks occur and by satisfying the Kutta–Joukowski condition for lift generation. The discrete variational problems associated with these equations are solved iteratively by a Buckley–Lenir algorithm[9] (preconditioned conjugate gradient method combined with a quasi-Newton method) and impressive results in CPU time are obtained compared with those obtained by a standard preconditioned conjugate gradient algorithm.

NUMERICAL RESULTS

We consider in this section the solution of various non-linear 2-D and 3-D transonic external flow problems by the stream vector correction method described in the second section. Previous results concerning, among others, subsonic rotational internal flows can be seen in References 1, 4, 6 and 10.

2-D transonic lifting/non-lifting cases

We present different 2-D non-lifting ($M_\infty = 0{\cdot}85$, $\alpha = 0°$) and lifting ($M_\infty = 0{\cdot}78$, $\alpha = 1°$) computations around a NACA0012 airfoil. These computations were done on a finite-element mesh having 2354 nodes and 4568 triangles, an enlargement of which is shown in Figure 4. For each test case, we compare the solution of the non-rotational potential scheme with the rotational correction one.

We can observe that the shock comes back towards the leading edge (Figures 5(a) and 6(a))

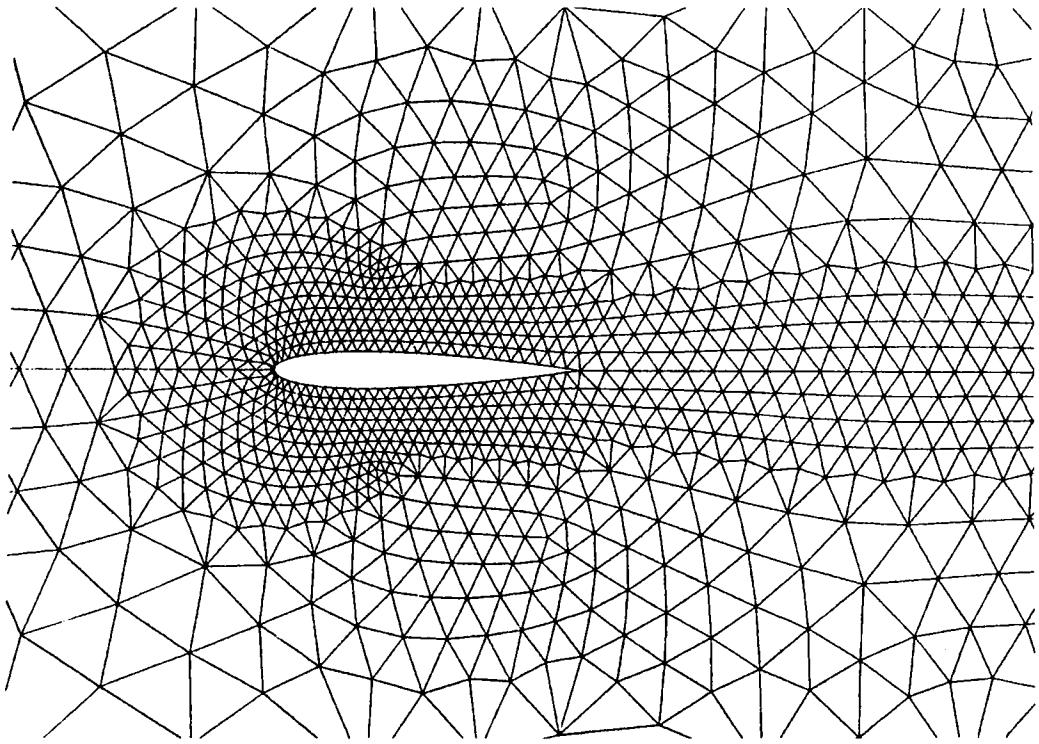

Figure 4

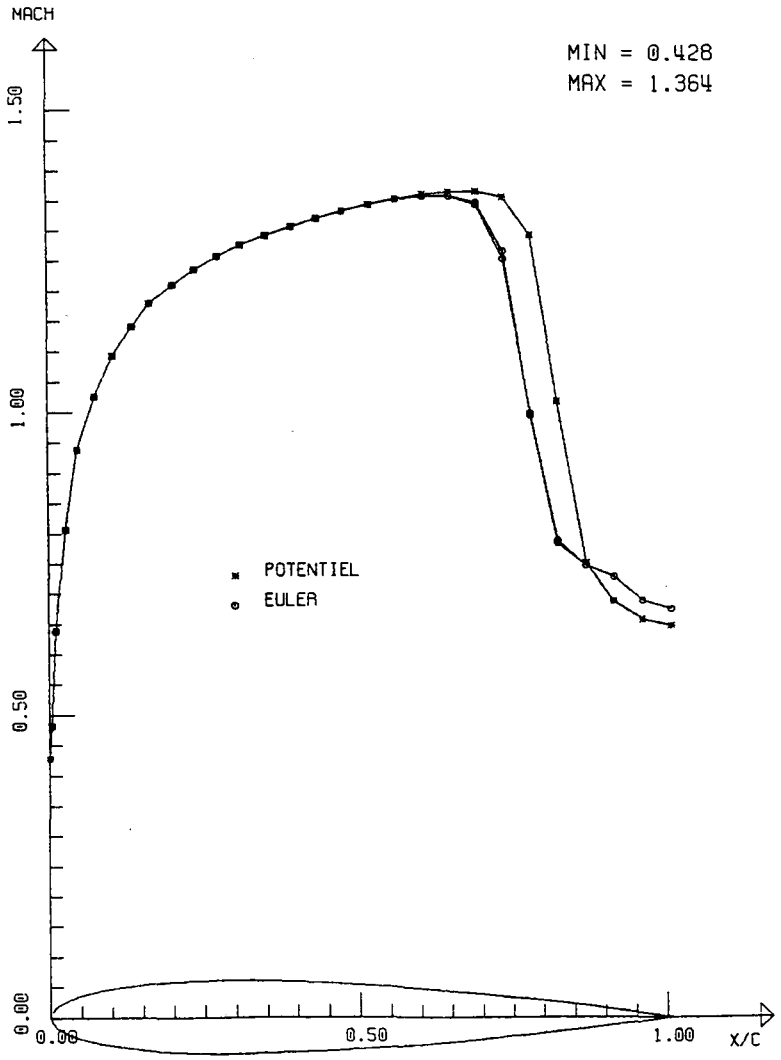

Figure 5(a). Mach distribution: angle of attack 0·00, free-stream Mach 0·85

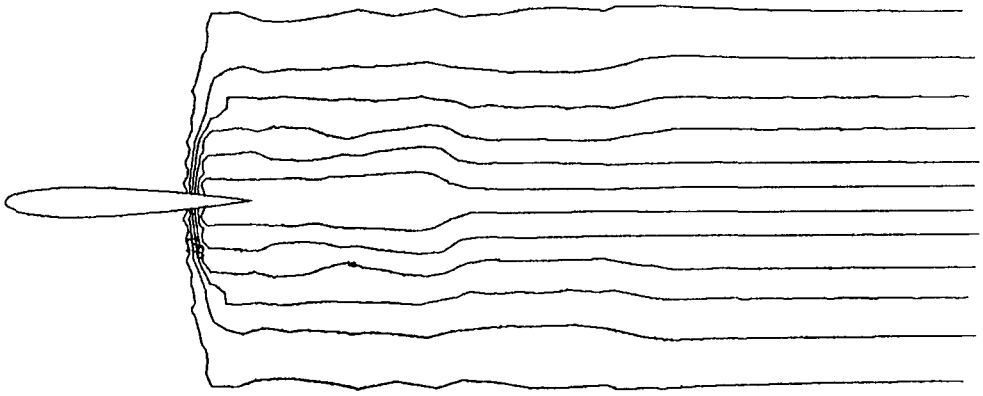

Figure 5(b). Isoentropy lines: angle of attack 0·00, free-stream Mach 0·85

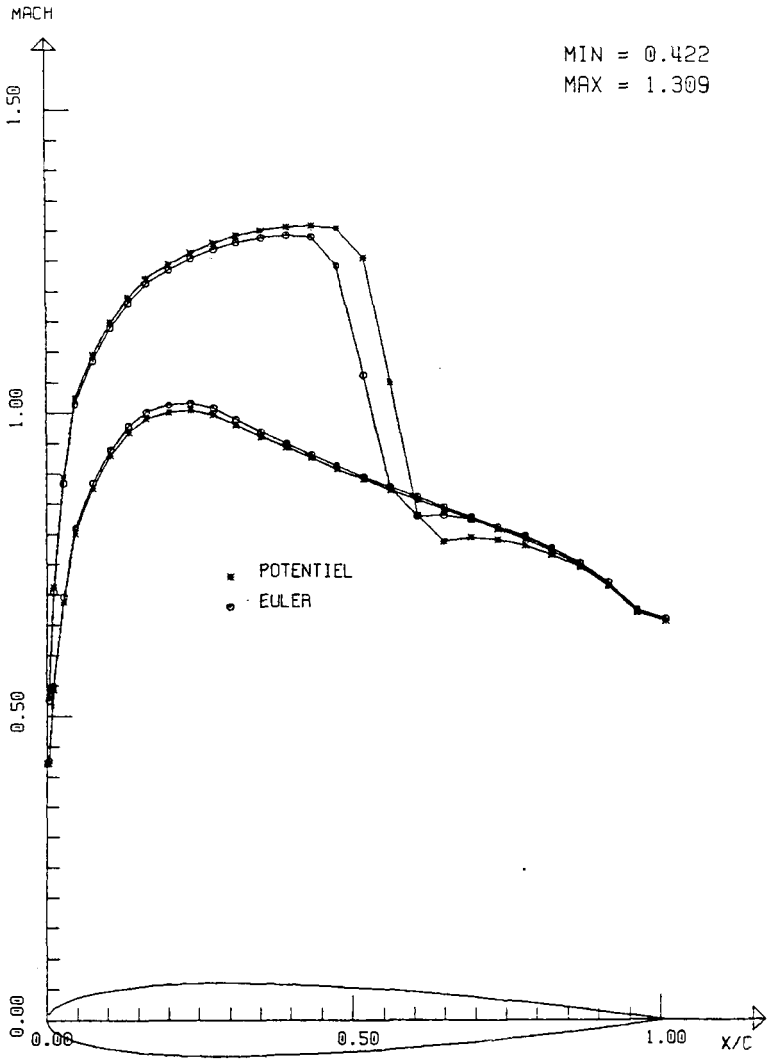

Figure 6(a). Mach distribution: angle of attack 1·00, free-stream Mach 0·78

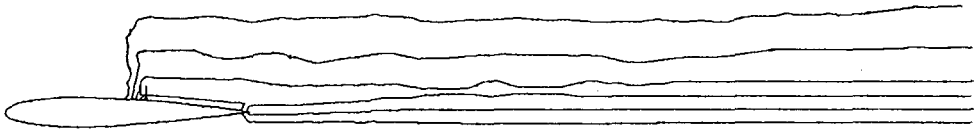

Figure 6(b). Isoentropy lines: angle of attack 1·00, free-stream Mach 0·78

in the two cases. The non-dissipative character of the scheme is illustrated by the isoentropy lines (Figures 5(b) and 6(b)).

If we want a computation at $M_\infty = 0{\cdot}85$ and $\alpha = 1°$, it is impossible to catch the potential solution because the Mach number at infinity is too large and the shock comes downstream to the trailing edge, with the result that the Kutta–Joukowski condition cannot be satisfied. Thus we use as initial guess the solution of the flow at $M_\infty = 0{\cdot}80$ and $\alpha = 1°$. In this way, it is possible

to reach the Euler potential solution. We present respectively in Figure 7(a) and 7(b) the Mach distribution and the isoentropy lines; we verify again the non-dissipative character of the entropy distribution.

Another interesting result is presented in Figure 8. It is possible to draw the curve CL function of the angle of attack for a given Mach number $M_\infty = 0{\cdot}83$; on this figure we perform with the transonic potential code multiple CL solutions for a given angle of attack, while the same computation with the ψ correction code shows a unique value of CL. The comparison seems to indicate that multiple solutions occur only for potential calculations.

3-D transonic lifting/non-lifting cases

We set two different computations around a NACA0012 wing between walls. The first is a non-lifting flow one at $M_\infty = 0{\cdot}85$ and $\alpha = 0°$. The second one is lifting at $M_\infty = 0{\cdot}85$ and $\alpha = 1°$.

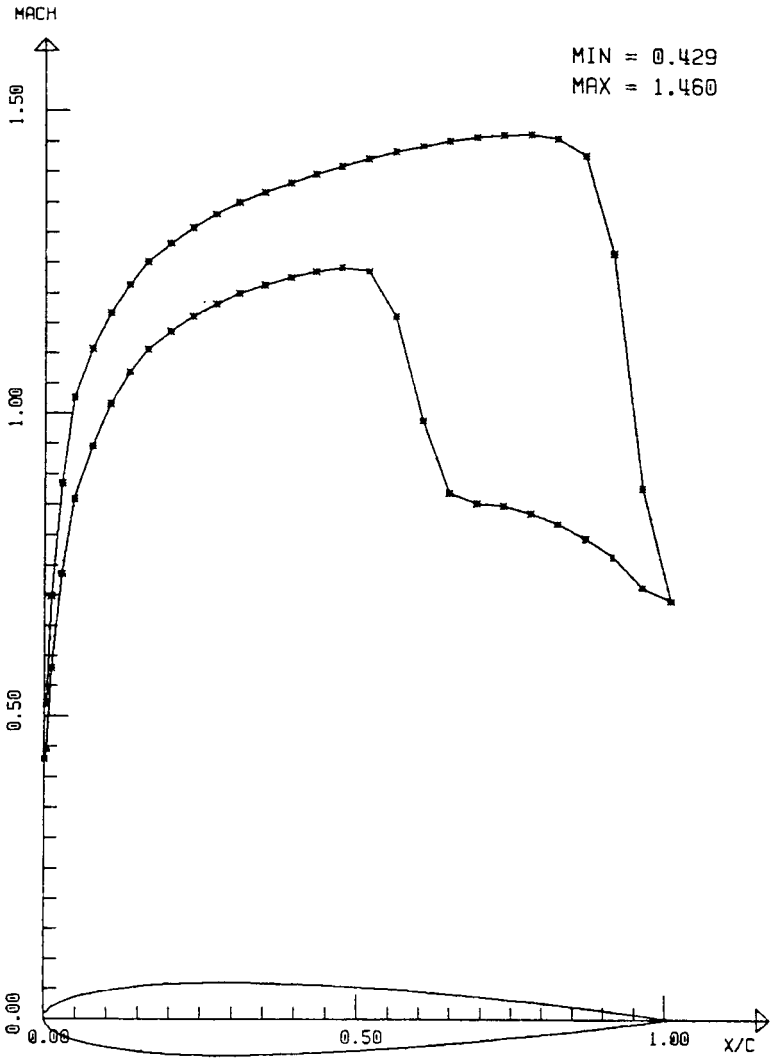

Figure 7(a). Mach distribution: angle of attack 1·00, free-stream Mach 0·85

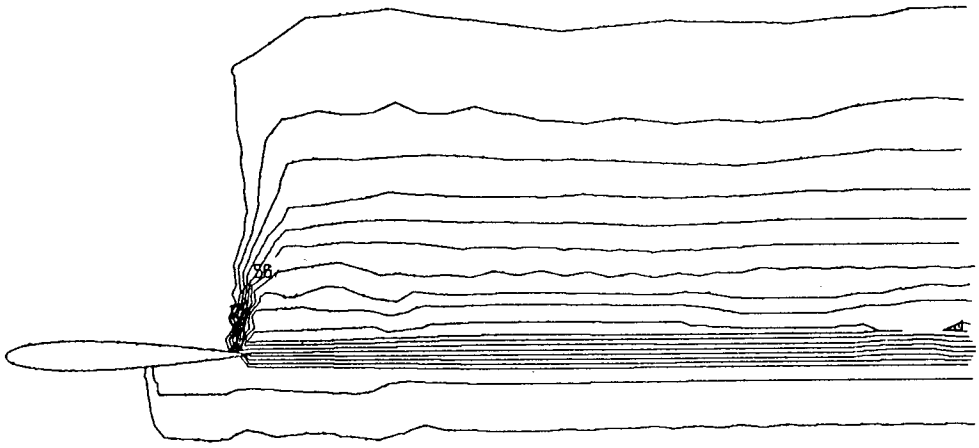

Figure 7(b). Isoentropy lines: angle of attack 1·00, free-stream Mach 0·85

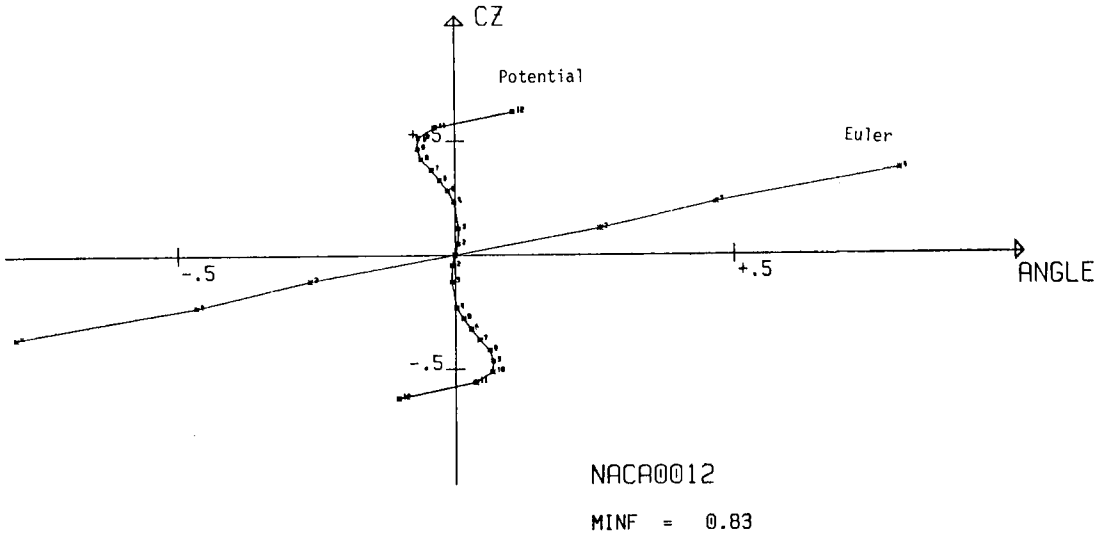

Figure 8. NACA0012: MINF = 0·83

For these two cases, we present respectively the entropy and the Mach distribution of the corrected velocity in Figures 9 and 11, and the entropy and the Mach level on the wing surface in Figures 10 and 12; as in 2-D, we verify again the non-dissipative character of the entropy distribution.

CONCLUSION

In both 2-D and 3-D computations, the comparison between the entropy level and the Mach distribution coming from Euler solutions and from our (ϕ–ψ) Euler solution point out the ability of this method to compute Euler flows without entropy dissipation. In all cases, we only need a few iterations (in practise two or three) to reach a satisfactory correction for the potential solution. Coupled with domain decomposition methodology, this modelling approach seems

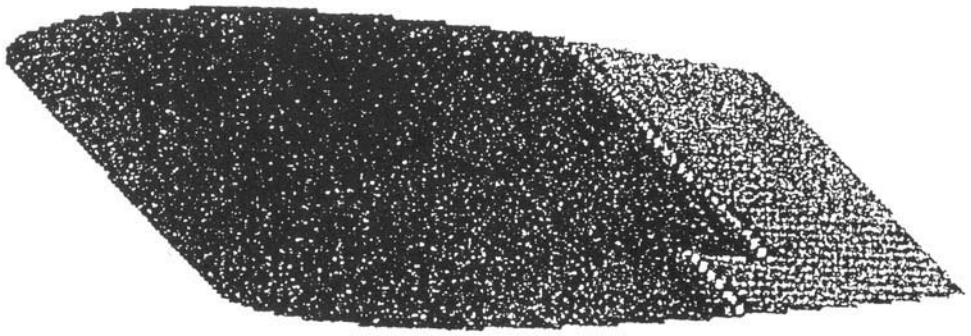

Entropy distribution

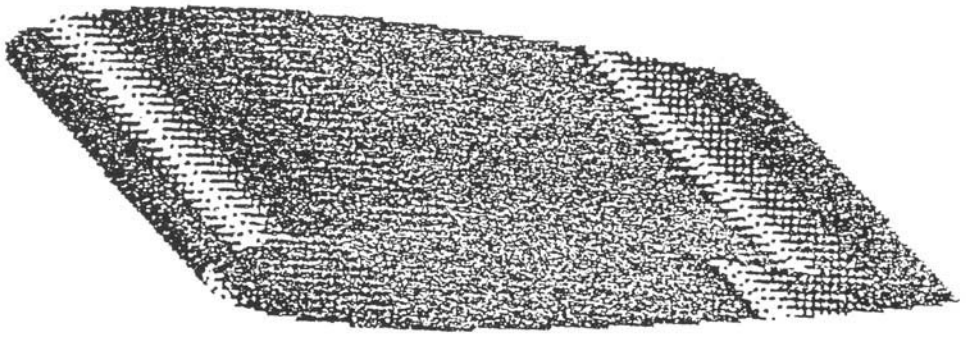

Mach distribution

Figure 9

attractive in terms of CPU time where the iterative process (ϕ–ψ) will be used only on selected subdomains of the flow.

ACKNOWLEDGEMENTS

This work was partly supported by STPA under Grant 84 95 00312. The authors thank Dr. P. Perrier of AMD/BA Industries and Professor R. Glowinski of INRIA for their stimulating and helpful suggestions.

NOTATION

Ω	Bounded domain of $\mathbb{R}^3(\mathbb{R}^2)$
Γ	$\Gamma_{in} \cup \Gamma_{out} \cup \Gamma_B$: boundary of Ω

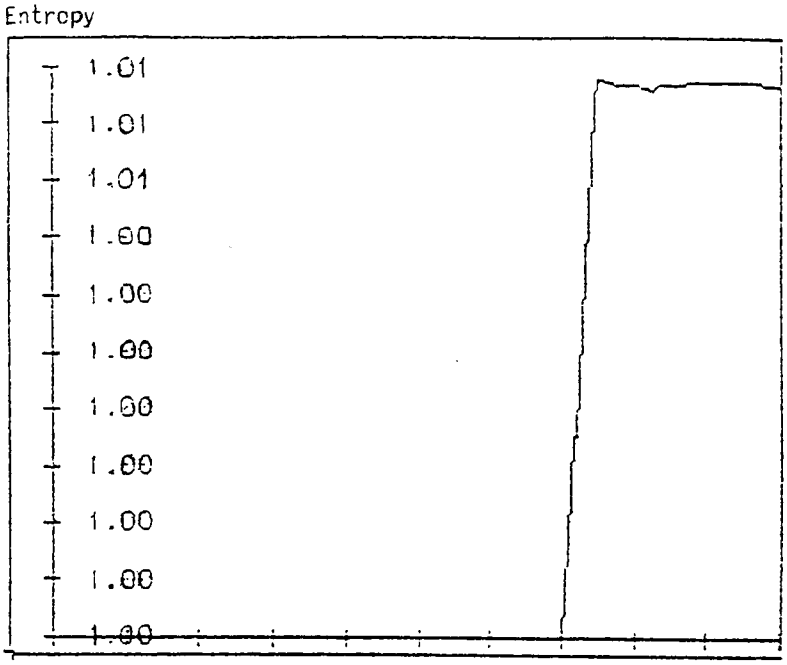
Entropy
1.01
1.01
1.01
1.00
1.00
1.00
1.00
1.00
1.00
1.00
1.00

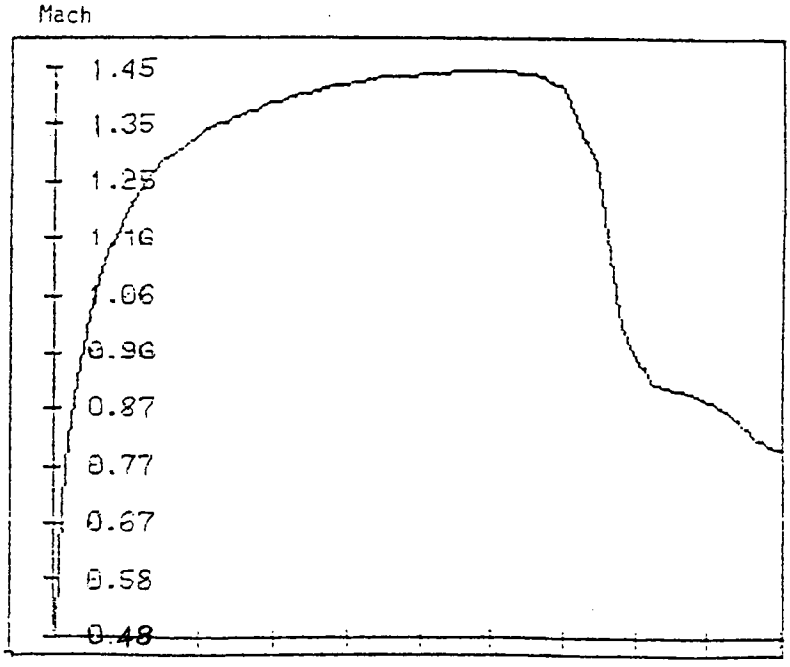
Mach
1.45
1.35
1.25
1.16
1.06
0.96
0.87
0.77
0.67
0.58
0.48

Figure 10

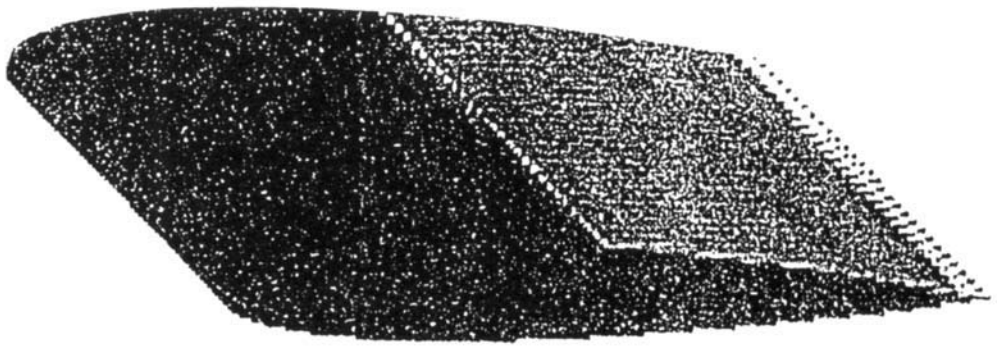

Entropy distribution

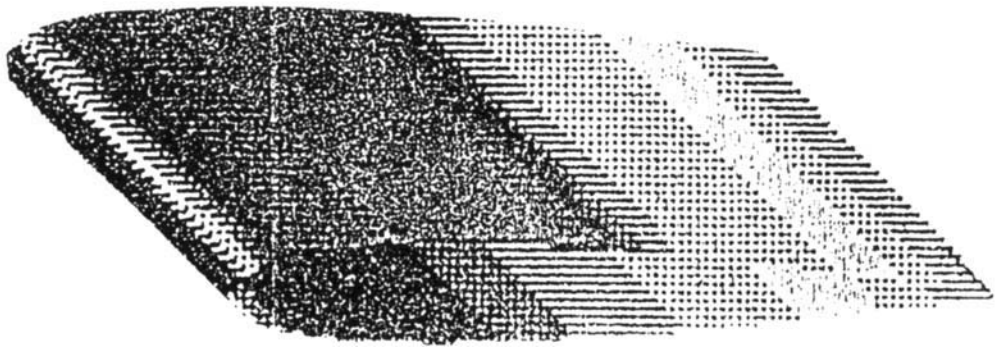

Mach distribution

Γ_{in}	Upstream boundary
Γ_{out}	Downstream boundary
Γ_B	Slip or body boundary
$\mathbf{n}$	Outward unit normal defined on Γ
$\mathbf{u}$	Velocity
ψ	Stream vector (or vector potential)
ϕ	Scalar potential
	Density
	Pressure
	Total energy

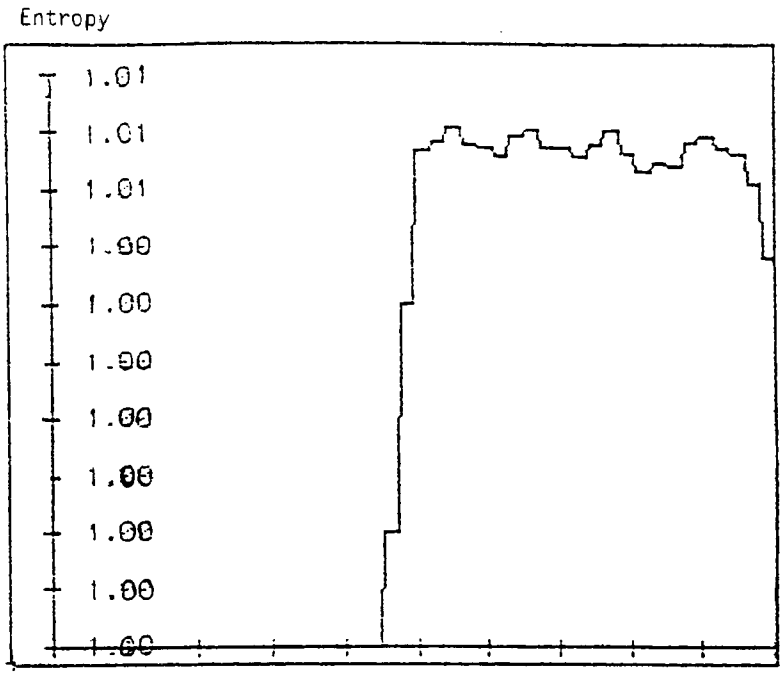
Entropy
1.01
1.01
1.01
1.00
1.00
1.00
1.00
1.00
1.00
1.00

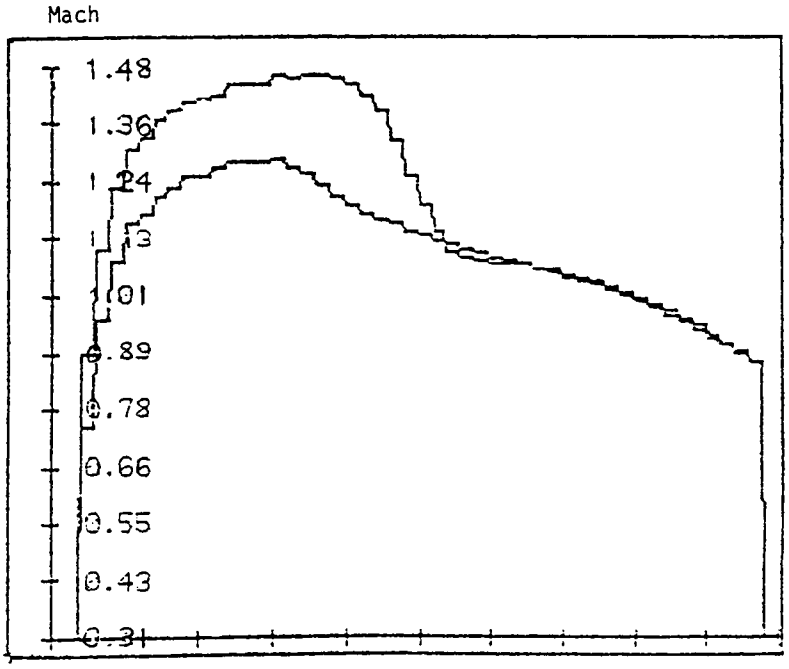
Mach
1.48
1.36
1.24
1.13
1.01
0.89
0.78
0.66
0.55
0.43
0.31

Figure 12

H	Total enthalpy
s	Specific entropy
S	Modified entropy
$\boldsymbol{\omega}$	Vorticity
γ	C_p/C_v, specific heat ratio ($\approx 1{\cdot}4$ for air)
$\nabla\cdot$	Divergence
∇	Gradient
Δ	Laplacian
∇x	Curl
$(\mathbf{u}\otimes\mathbf{v})_{ij}$	$\mathbf{u}_i\mathbf{v}_j$ (tensor product)
$\mathbf{u}\times\mathbf{v}$	Cross product between $\mathbf{u}$ and $\mathbf{v}$
$\mathbf{u}\cdot\mathbf{v}$	Inner product between $\mathbf{u}$ and $\mathbf{v}$
$(\mathbf{u},\mathbf{v})$	Inner product between $\mathbf{u}$ and $\mathbf{v}$ in $\mathbf{L}^2(\Omega)$, $\|\cdot\|_{0,\Omega}$ the associated norm
$\mathbf{H}^1(\Omega)$	$\{w\in\mathbf{L}^2(\Omega):\nabla w\in(\mathbf{L}^2(\Omega))^3\}$
$\|w\|_{1,\Omega}$	$(\|w\|^2_{0,\Omega}+\|\nabla w\|^2_{0,\Omega})^{1/2}$, the $\mathbf{H}^1(\Omega)$ norm
$\mathbf{H}^1(\Omega)/\mathbb{R}$	$\{\mathbf{H}^1(\Omega)$ quotiented by the constants$\}$
$(\mathbf{n},\mathbf{s}_1,\mathbf{s}_2)$	Local orthonormal positive direct co-ordinate system defined on Γ with $(\mathbf{s}_1,\mathbf{s}_2)$ tangent to Γ and orthogonal to $\mathbf{n}$.

REFERENCES

1. F. El Dabaghi, *Thèse de 3ème cycle*, University of Paris XIII, 1984.
2. F. El Dabaghi and O. Pironneau, 'Stream vectors in the three-dimensional aerodynamics', *Numer. Math.*, **48,** 561–589 (1986).
3. C. Bernardi, *Thèse de 3ème cycle*, University of Paris VI, 1979.
4. F. El Dabaghi and G. Poirier, *Internal Report*, INRIA, 1987.
5. O. Pironneau, 'On the transport diffusion algorithm and its applications to the Navier–Stokes equations', *Numer. Math.*, **8,** 309–332 (1980).
6. F. El Dabaghi, J. Periaux, O. Pironneau and G. Poirier, '3-D finite element solution of steady Euler transonic flow by stream vector correction', *Proc. AIAA 7th CFD Conference*, Cincinnati, Ohio, U.S.A., 15–17 July 1985.
7. G. Poirier, *Thèse de 3ème cycle*, University of Paris VI, 1981.
8. M. O. Bristeau, R. Glowinski, J. Periaux, P. Perrier, O. Pironneau and G. Poirier, 'On the numerical solution of non-linear problems in fluid dynamics by least squares and finite element methods (II). Application to transonic flow simulations', *Comp. Meth. Appl. Mech. Eng.*, **51,** (1985).
9. A. Buckley and A. Lenir, 'QN-like variable storage conjugate gradients', *Math. Programming*, **27,** 155–175 (1983).
10. *GAMM Workshop on Numerical Simulation of Compressible Euler Flows*, Rocquencourt, France, 10–13 June 1986.